



ELSEVIER

Available online at [www.sciencedirect.com](http://www.sciencedirect.com)

SCIENCE @ DIRECT®

Ocean Engineering 33 (2006) 82–92

OCEAN  
ENGINEERING

[www.elsevier.com/locate/oceaneng](http://www.elsevier.com/locate/oceaneng)

# Bragg resonant reflection of carrier waves composing wave groups

Yong-Sik Cho<sup>a,\*</sup>, Jae-Sang Jung<sup>b,1</sup>

<sup>a</sup>*Department of Civil Engineering, Hanyang University,  
17 Haengdang-dong, Seongdong-gu, Seoul 133-791, South Korea*

<sup>b</sup>*Civil Engineering Team, Hyundai Development Company,  
160 Samsung-dong, Gangnam-gu, Seoul 135-881, South Korea*

Received 21 September 2004; accepted 8 March 2005

Available online 1 July 2005

---

## Abstract

Numerical analyses for the Bragg resonant reflection of carrier waves associated long waves due to sinusoidally varying seabeds are performed by using a set of coupled ordinary differential equations derived from the Boussinesq equations. The Boussinesq equations are firstly approximated with the Fourier decomposition. The coupled governing equations are then derived and used to simulate evolution of both short and long wave components. It is also found that wave groups are generated by two carrier waves with slightly different frequencies. The wave energy of the initial wave components is transferred to other harmonic components during propagation over a long distance. Evolution and reflection of both short and long waves were largely affected by nonlinearity. © 2005 Elsevier Ltd. All rights reserved.

*Keywords:* Bragg resonant reflection; Boussinesq equations; Carrier waves; Wave group; Nonlinearity

---

## 1. Introduction

Water waves observed in shallow-water region are much irregular and simultaneously regular for a long time period. In general, short waves have periods of 3–15 s, while wave groups composed by carrier waves and long waves associated with wave groups have periods of 30 s to a few minutes (Liu and Cho, 1993). Long waves generated by wave

---

\* Corresponding author. Tel.: +82 2 2220 0393; fax: +82 2 2293 9977.

E-mail addresses: [ysc59@hanyang.ac.kr](mailto:ysc59@hanyang.ac.kr) (Y.-S. Cho), [finjon@hyundai-dvp.com](mailto:finjon@hyundai-dvp.com) (J.-S. Jung).

<sup>1</sup> Tel.: +82 22 008 8931; fax: +82 22 008 9011.

groups are called infragravity waves and these long period waves are believed to be responsible for harbor resonance and formation of rippled sand bars (Bowers, 1977; Mei and Agnon, 1989; Mei and Liu, 1993).

Since the laboratory demonstration by Heathershaw (1982), the Bragg resonant reflection has been studied by many researchers. Kirby (1986) calculated the Bragg reflection of propagating waves over sinusoidal and doubly sinusoidal seabeds. Yoon and Liu (1987) studied the near resonant reflection of cnoidal waves in shallow water with a couple of governing equations derived from the Boussinesq equations. Guazzelli et al. (1992) studied a higher order Bragg reflection. They carried out laboratory experiments for reflection of surface waves by doubly sinusoidally rippled beds. Liu et al. (1992) analyzed evolution of long waves generated by wave groups and shoaling effects with the Boussinesq equations. Liu and Cho (1993) studied the Bragg reflection of infragravity waves. They considered the reflection of long waves additionally and studied Bragg reflection of long waves generated by wave groups with a multiple-scale perturbation approach. They also showed that long waves associated with a wave group could be resonantly reflected by a sinusoidally varying topography. However, they neglected the reflection of short wave components.

Recently, Cho and Lee (2000) studied the Bragg reflection with the eigen function expansion method. They included evanescent modes created by a rippled bed. Arduin and Herbers (2002) investigated the Bragg reflection of random waves propagating over the irregular bottom topography. Cho and Lee (2003) extended Yoon and Liu's (1987) study by including fast varying terms and beach slope effects.

In this study, the Boussinesq equations derived by Peregrine (1967) were employed as the governing equations. The Boussinesq equations are well known to describe weakly nonlinear, weakly dispersive shallow-water waves. Following to Liu and Cho (1993), long and short wave components were not divided mathematically in this study. Incident waves were assumed to be long waves having an angular frequency of magnitude of  $\Omega$  as compared with the nondimensional angular frequency of short waves. Thus, the higher order terms of long wave components represent short waves. Furthermore, waves satisfying the condition of  $n\Omega \geq 1.0$  are regarded as short waves and investigated the strong reflection of carrier (short) waves composing wave groups.

A brief derivation of the governing equations is firstly introduced for completeness in the Section 2. Numerical example is given in Section 3. Particular attention is paid to the characteristics of the Bragg reflection of carrier waves composing wave groups. Finally, careful discussion on the solutions and concluding remarks are made in Section 4.

## 2. Modulation equations

In this section, a set of modulation equations for groups of sea swells in shallow water is derived from the one-dimensional Boussinesq equations. By employing  $\omega_0$  as the characteristic short wave frequency,  $a_0$  as the characteristic short wave amplitude, and  $h_0$  as the characteristic water depth, the following dimensionless variables may be

introduced as

$$t = \omega_0 t', \quad x = \frac{\omega_0}{\sqrt{gh}} x', \quad h = \frac{1}{h_0} h', \quad u = \frac{h_0}{a_0(g h_0)^{1/2}} u', \quad \zeta = \frac{1}{a_0} \zeta',$$

$$\omega = \frac{1}{\omega_0} \omega'$$
(1)

where  $\xi$  is the free surface displacement,  $u$  denotes the depth-averaged horizontal velocity, and  $g$  denotes the gravitational acceleration.

Using these dimensionless variables, the Boussinesq equations can be written in the following dimensionless form (Liu and Cho, 1993; Cho and Lee, 2003).

$$\frac{\partial \zeta}{\partial t} + \frac{\partial}{\partial x} [(h + \varepsilon \zeta)u] = 0$$
(2)

$$\frac{\partial u}{\partial t} + \varepsilon u \frac{\partial u}{\partial x} + \frac{\partial \zeta}{\partial x} = \mu^2 \left[ \frac{1}{2} h \frac{\partial^2}{\partial x^2} \left( h \frac{\partial u}{\partial t} \right) - \frac{1}{6} h^2 \frac{\partial^2}{\partial x^2} \left( \frac{\partial u}{\partial t} \right) \right] + O(\varepsilon^2, \varepsilon \mu^2, \mu^4)$$
(3)

where

$$\varepsilon = \frac{a_0}{h_0} \ll 1, \quad \mu^2 = \frac{\omega_0^2 h_0}{g} \ll 1$$
(4)

and  $\varepsilon$  and  $\mu^2$  are small parameters representing the nonlinearity and frequency dispersion, respectively.

To investigate reflection and shoaling of incident waves over a slowly varying topography, the water depth is described as (Fig. 1)

$$h = \bar{h} + \tilde{h}$$
(5)

in which  $O\left(\frac{dh}{dx}\right) \approx O(\mu^2)$  has been assumed.

Assuming a periodic motion in time, the free surface displacement and the horizontal velocity can be expressed as Fourier series given by

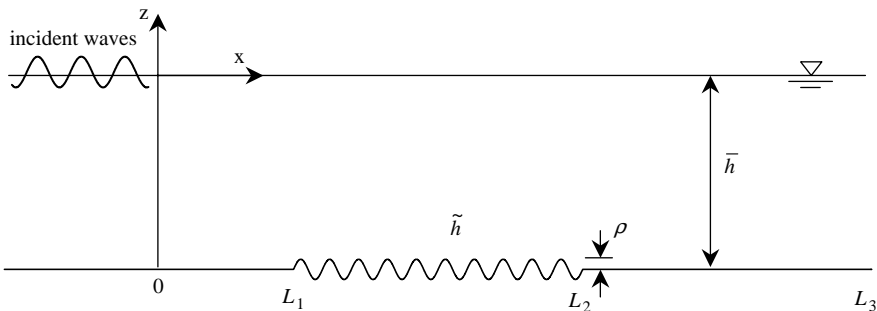


Fig. 1. A definition sketch of a slowly varying seabed.

$$\zeta(x, t) = \frac{1}{2} \sum_n \zeta_n(x) e^{-i\Omega t}, \quad u(x, t) = \frac{1}{2} \sum_n u_n(x) e^{-i\Omega t} \quad (6)$$

with  $n=0, \pm 1, \pm 2$ . By differentiating Eq. (7) with respect to  $x$  and  $t$ , the following relations can be obtained

$$\frac{\partial \zeta}{\partial t} = -\frac{i\Omega}{2} \sum_n n \zeta_n e^{-i\Omega t}, \quad \frac{\partial \zeta}{\partial x} = \frac{1}{2} \sum_n \frac{d\zeta_n}{dx} e^{-i\Omega t}, \quad (7)$$

$$\frac{\partial u}{\partial t} = -\frac{i\Omega}{2} \sum_n n u_n e^{-i\Omega t}, \quad \frac{\partial u}{\partial x} = \frac{1}{2} \sum_n \frac{du_n}{dx} e^{-i\Omega t}$$

By substituting Eqs. (5)–(7) into Eqs. (2) and (3) and collecting the  $n$ th Fourier components, the followings can be derived

$$-i\Omega n \zeta_n + \frac{d}{dx}(h u_n) + \frac{\varepsilon}{2} \sum_s \frac{d}{dx}(\zeta_s u_{n-s}) = 0 \quad (8)$$

$$-i\Omega n u_n + \frac{\varepsilon}{4} \sum_s \frac{d}{dx}(u_s u_{n-s}) + \frac{d\zeta_n}{dx} = -\frac{1}{3} i n \mu^2 \Omega \bar{h}^2 \frac{d^2 u_n}{dx^2} + O(\varepsilon^2, \varepsilon \mu^2, \mu^4) \quad (9)$$

where  $s=0, \pm 1, \pm 2, A$ . The leading order terms of Eqs. (8) and (9) yield

$$\zeta_n = -\frac{i\bar{h}}{n\Omega} \frac{du_n}{dx} + O(\varepsilon), \quad u_n = -\frac{i}{n\Omega} \frac{d\zeta_n}{dx} + O(\varepsilon) \quad (10)$$

for  $n \neq 0$  and

$$\zeta_0 = -\frac{\varepsilon}{4} \sum_s u_s u_{-s} + O(\varepsilon^2), \quad u_0 = -\frac{\varepsilon}{2\bar{h}} \sum_s \zeta_s u_{-s} + O(\varepsilon^2) \quad (11)$$

for  $n=0$ . Eq. (11) represents steady components which do not have any contributions to other harmonics up to  $O(\varepsilon)$ . Thus, the steady components are not considered in this study.

Combining the continuity and the momentum equations, the following equation can be derived.

$$\begin{aligned} n^2 \Omega^2 \zeta_n + \frac{dh}{dx} \frac{d\zeta_n}{dx} + \frac{\varepsilon n}{2} \sum_{s \neq 0, n} \frac{d}{dx} \left\{ \frac{1}{n-s} \left( \frac{d\zeta_{n-s}}{dx} \right) \right\} + \frac{1}{3} \mu^2 \bar{h}^3 \frac{d^4 \zeta_n}{dx^4} \\ - \frac{\varepsilon \bar{h}}{4} \sum_{s \neq 0, n} \frac{1}{(n-s)s} \frac{d^2}{dx^2} \left( \frac{d\zeta_s}{dx} \frac{d\zeta_{n-s}}{dx} \right) + h \frac{d^2 \zeta_n}{dx^2} = O(\varepsilon^2, \varepsilon \mu^2, \mu^4) \end{aligned} \quad (12)$$

The leading order of Eq. (12) yields

$$\frac{d^2 \zeta_n}{dx^2} = -\frac{n^2 \Omega^2}{\bar{h}} \zeta_n + O(\varepsilon) \quad (13)$$

Eq. (13) is the linear wave equation and can be solved as

$$\zeta_n \sim \left[ \exp\left(in\Omega \int \frac{1}{\sqrt{h}} dx\right), \exp\left(-in\Omega \int \frac{1}{\sqrt{h}} dx\right) \right] \quad (14)$$

By using Eq. (13), Eq. (12) may be rewritten as

$$\begin{aligned} & \bar{h} \frac{d^2 \zeta_n}{dx^2} + \frac{dh}{dx} \frac{d\zeta_n}{dx} + n^2 \Omega^2 \left( 1 - \frac{\tilde{h}}{\bar{h}} + \frac{1}{3} \mu^2 n^2 \Omega^2 \bar{h} \right) \zeta_n \\ &= \frac{\varepsilon \Omega^2}{2\bar{h}} \sum_{s \neq 0, n} \{ n^2 - (1 - \Omega^2) - s^2 \Omega^2 \} \zeta_s \zeta_{n-s} - \frac{\varepsilon}{2} \sum_{s \neq 0, n} \frac{n + \Omega^2 s}{n - s} \frac{d\zeta_s}{dx} \frac{d\zeta_{n-s}}{dx} \\ &+ O(\varepsilon^2, \varepsilon \mu^2, \mu^4) \end{aligned} \quad (15)$$

Following Liu and Cho’s (1993) approach, the wave field can be split into the right- and the left-going wave components as:

$$\zeta_n = \zeta_n^+ + \zeta_n^- \quad (16)$$

in which  $\zeta_n^+$  and  $\zeta_n^-$  denote the right and the left-going wave components, respectively. Then, the following coupled equations have been assumed

$$\frac{d\zeta_n^+}{dx} = \frac{in\Omega}{\sqrt{h}} \zeta_n^+ + Fn, \quad \frac{d\zeta_n^-}{dx} = -\frac{in\Omega}{\sqrt{h}} \zeta_n^- - Fn \quad (17)$$

where the coupling term  $Fn$  is to be determined. By substituting Eqs. (16) and (17) into Eq. (15) and after a lengthy algebra, the coupling term can be determined as

$$\begin{aligned} Fn &= -\frac{1}{2\bar{h}} \left[ \frac{1}{2} \frac{d\bar{h}}{dx} + \frac{d\tilde{h}}{dx} \right] (\zeta_n^+ - \zeta_n^-) + \frac{in\Omega}{2\sqrt{h}} \left[ -\frac{\tilde{h}}{\bar{h}} + \frac{\mu^2 n^2 \Omega^2 \sqrt{\bar{h}}}{3} \right] (\zeta_n^+ + \zeta_n^-) \\ &- \frac{i\varepsilon \Omega}{4\bar{h}\sqrt{h}} \sum_{s \neq 0, n} (n + s\Omega^2) [\zeta_s^+ \zeta_{n-s}^+ + \zeta_s^- \zeta_{n-s}^-] - \frac{i\varepsilon \Omega}{4\bar{h}\sqrt{h}} \sum_{s \neq 0, n} \frac{n - 2s}{n} (n \\ &+ s\Omega^2) [\zeta_s^+ \zeta_{n-s}^- + \zeta_s^- \zeta_{n-s}^+] + O(\varepsilon^2, \varepsilon \mu^2, \mu^4) \end{aligned} \quad (18)$$

After assuming a periodic motion in space again, the wave components can be expressed as

$$\zeta_n^+ = A_n(x) e^{in\Omega\theta}, \quad \zeta_n^- = B_n(x) e^{-in\Omega\theta} \quad (19)$$

in which  $\theta = \int \frac{1}{\sqrt{h}} dx$  has been used. By differentiating Eq. (19) with respect to  $x$ , the following relations are obtained.

$$\frac{d\zeta_n^+}{dx} = \frac{dA_n}{dx} e^{in\Omega\theta} + \frac{in\Omega}{\sqrt{h}} A_n e^{in\Omega\theta}, \quad \frac{d\zeta_n^-}{dx} = \frac{dB_n}{dx} e^{-in\Omega\theta} - \frac{in\Omega}{\sqrt{h}} B_n e^{-in\Omega\theta} \quad (20)$$

Substituting Eqs. (18)–(20) into Eq. (17) yields a set of coupled nonlinear first-order

ordinary differential equations given as

$$\begin{aligned} \frac{dA_n}{dx} = & \left( -\frac{1}{4\bar{h}} \frac{d\bar{h}}{dx} - \frac{1}{2\bar{h}} \frac{d\tilde{h}}{dx} - \frac{in\Omega\tilde{h}}{2\bar{h}\sqrt{\bar{h}}} + \frac{i\mu^2 n^3 \Omega^3 \sqrt{\bar{h}}}{6} \right) A_n \\ & + \left( \frac{1}{4\bar{h}} \frac{d\bar{h}}{dx} + \frac{1}{2\bar{h}} \frac{d\tilde{h}}{dx} - \frac{in\Omega\tilde{h}}{2\bar{h}\sqrt{\bar{h}}} + \frac{i\mu^2 n^3 \Omega^3 \sqrt{\bar{h}}}{6} \right) B_n e^{-2in\Omega\theta} - \frac{\varepsilon i\Omega}{4\bar{h}\sqrt{\bar{h}}} \\ & \times \sum_{s \neq 0, n} (n + s\Omega^2) [A_s A_{n-s} + B_s B_{n-s} e^{-2in\Omega\theta}] - \frac{\varepsilon i\Omega}{4\bar{h}\sqrt{\bar{h}}} \\ & \times \sum_{s \neq 0, n} \frac{n - 2s}{n} (n + s\Omega^2) [A_s B_{n-s} e^{-2i(n-s)\Omega\theta} + B_s A_{n-s} e^{-2is\Omega\theta}] + O(\varepsilon^2, \varepsilon\mu^2, \mu^4) \end{aligned} \tag{21}$$

for the right-going waves, and

$$\begin{aligned} \frac{dB_n}{dx} = & \left( -\frac{1}{4\bar{h}} \frac{d\bar{h}}{dx} - \frac{1}{2\bar{h}} \frac{d\tilde{h}}{dx} + \frac{in\Omega\tilde{h}}{2\bar{h}\sqrt{\bar{h}}} - \frac{i\mu^2 n^3 \Omega^3 \sqrt{\bar{h}}}{6} \right) B_n \\ & + \left( \frac{1}{4\bar{h}} \frac{d\bar{h}}{dx} + \frac{1}{2\bar{h}} \frac{d\tilde{h}}{dx} - \frac{in\Omega\tilde{h}}{2\bar{h}\sqrt{\bar{h}}} + \frac{i\mu^2 n^3 \Omega^3 \sqrt{\bar{h}}}{6} \right) A_n e^{2in\Omega\theta} + \frac{\varepsilon i\Omega}{4\bar{h}\sqrt{\bar{h}}} \\ & \times \sum_{s \neq 0, n} (n + s\Omega^2) [A_s A_{n-s} e^{2in\Omega\theta} + B_s B_{n-s}] + \frac{\varepsilon i\Omega}{4\bar{h}\sqrt{\bar{h}}} \sum_{s \neq 0, n} \frac{n - 2s}{n} \\ & \times (n + s\Omega^2) [A_s B_{n-s} e^{2is\Omega\theta} + B_s A_{n-s} e^{2i(n-s)\Omega\theta}] + O(\varepsilon^2, \varepsilon\mu^2, \mu^4) \end{aligned} \tag{22}$$

for the left-going waves. Once  $A_n$  and  $B_n$  are determined, the free surface displacement can be recovered from Eqs. (7) and (19). That is,

$$\zeta(x, t) = \frac{1}{2} \sum_n [A_n e^{in\Omega\theta} + B_n e^{-in\Omega\theta}] e^{-in\Omega t} \tag{23}$$

### 3. Numerical example

In this section, numerical results for the propagation and reflection of carrier waves composing wave groups by a sinusoidally varying bottom topography are presented. The coupled nonlinear governing equations for waves derived in the previous section are integrated by using the fourth-order Runge-Kutta method. Eqs. (21) and (22) should be solved simultaneously with prescribed boundary and initial conditions for  $A_n$ .

An iterative scheme is adopted from Liu and Cho (1993) to solve the governing equations. In the scheme, the transmitted wave field is first solved without consideration of a reflected wave field. The reflected wave is then calculated with transmitted wave

solutions. The transmitted wave field is finally updated with the newly obtained reflected wave field. This procedure is repeated until converged solutions are obtained. The convergence condition is defined as

$$\frac{||A_n|^k - |A_n|^{k-1}|}{|A_n|^{k-1}} < 10^{-4}, \quad \frac{||B_n|^k - |B_n|^{k-1}|}{|B_n|^{k-1}} < 10^{-4} \tag{24}$$

where  $k-1$  and  $k$  represent a previous and a current iteration steps, respectively.

Fig. 2 shows the propagation of carrier waves composing wave groups and evolution of long wave components. The following initial conditions are employed for carrier waves.

$$A_n = 1.0, \quad A_{n+1} = 1.0 \quad (n\Omega \approx 1) \tag{25}$$

in which  $n$  is equal to 10 because the value of  $\Omega$  is 0.1 in Fig. 2. In the first example, numerical results are obtained for  $\rho = 0.12$  and  $\delta = 2.0$ . The rippled bed begins at  $x(=L_1) = 70\pi$  and ends at  $x(=L_2) = 80\pi$ . Therefore, there are 10 sinusoidal ripples within the ripple bed. In both Figs.,  $n_{\max} = 20$  is used, and the frequency of a wave group represented by  $\Omega$

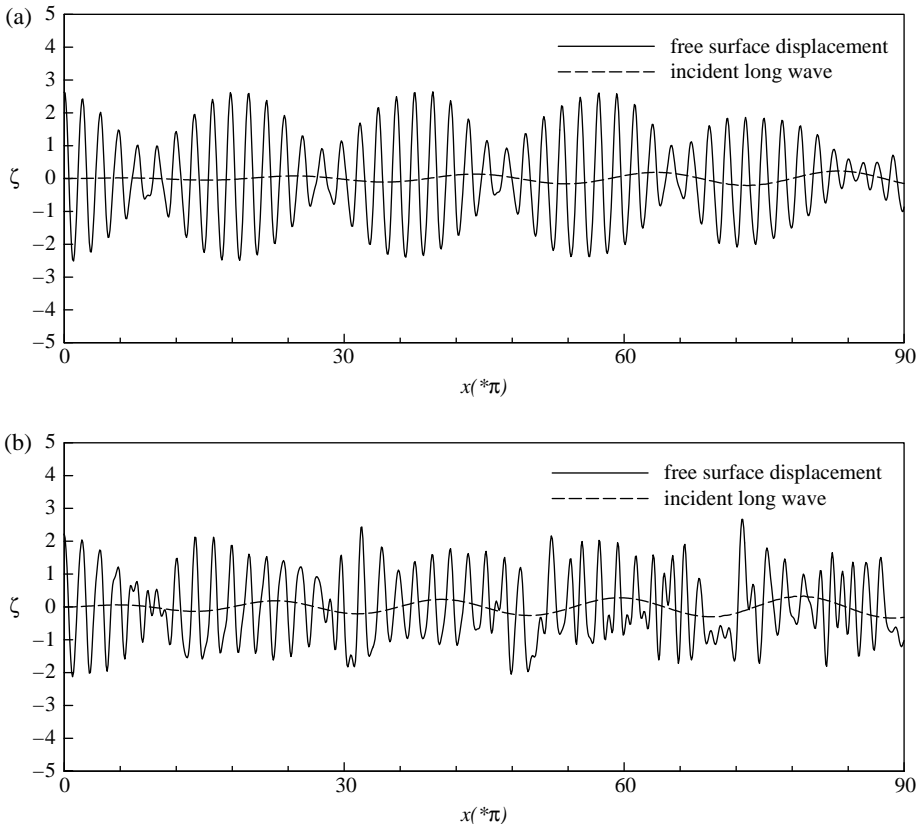


Fig. 2. The evolution of wave groups and transmitted long waves over a rippled bed: (a)  $\epsilon = 0.02, \mu^2 = 0.1$ ; (b)  $\epsilon = 0.08, \mu^2 = 0.1$ .

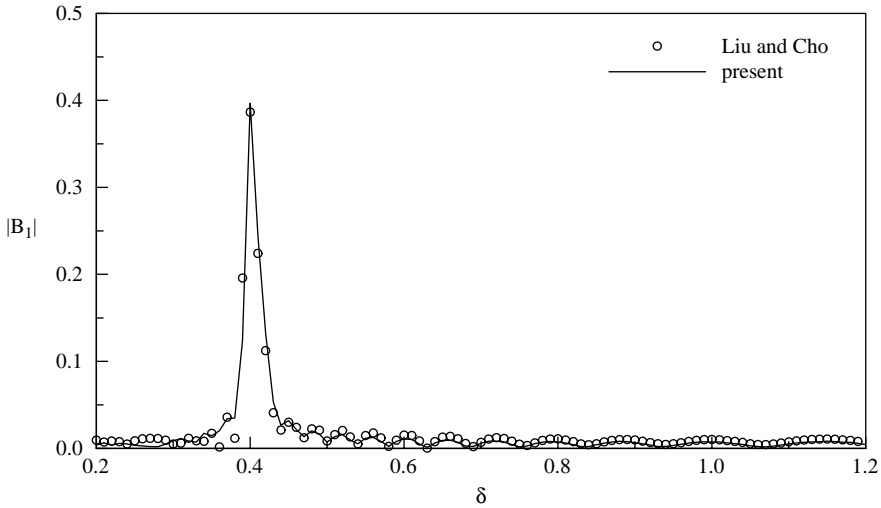


Fig. 3. Bragg reflection of long waves ( $p=0.08$ ,  $n=20$ ,  $\Omega=0.2$ ,  $\varepsilon=0.02$ ,  $\mu^2=0.09$ ).

is 0.1. In Fig. 2, free surface profiles and the transmitted long waves over the rippled bed at  $t=0$  are presented. The amplitude of the transmitted long waves in Fig. 2(b) is larger than that of Fig. 2(a). In Fig. 2(a) and (b), the free surface profile becomes more irregular and noisy as the nonlinearity increases. That is, more energy transfers to other harmonic components as the nonlinearity increases due to active interactions among other harmonic components.

To ensure the accuracy of the numerical scheme used for integrating Eqs. (21) and (22), numerical solutions for the Bragg reflection of long waves are first obtained and compared to those by Liu and Cho (1993). As shown in Fig. 3, the numerical solutions for long waves agree very well. Thus, the present model can be applicable for long waves associated with the wave groups. The present model includes reflections of short wave components as well as long wave components. However, Liu and Cho considered reflection of only long wave components. Thus, Liu and Cho's study can be viewed as a limiting case of the present study.

Fig. 4 shows incident and reflected wave profiles propagating over the rippled bed connected two equally constant depth regions. The rippled zone begins at  $x=70\pi$  and ends at  $x=90\pi$ . The conditions of the rippled seabed are also the Bragg reflection condition for incident carrier waves. When the nonlinearity is relatively small, the reflected wave amplitude increases for a less amount of energy transfer from initial wave components to others. The magnitude of resonant effects of carrier waves is also appreciable.

Nextly, the Bragg resonant reflection with a fixed length of a rippled bed is investigated. The wavelength of a ripple varies as the wavenumber varies and the rippled bed begins at  $x=L_1=70\pi$  with  $n_{\max}=30$ . Fig. 5 shows the amplitude spectrum of the wave group at  $x=70\pi$ . Energy is transferred to the other harmonic components from the initial conditions  $A_{10}$  and  $A_{11}$  due to nonlinear interactions among other components.

Figs. 6 and 7 show the energy of reflected wave components of carrier waves with  $\varepsilon=0.02$ ,  $\mu^2=0.1$  and  $\varepsilon=0.08$ ,  $\mu^2=0.1$  respectively. The wave energy is proportional to

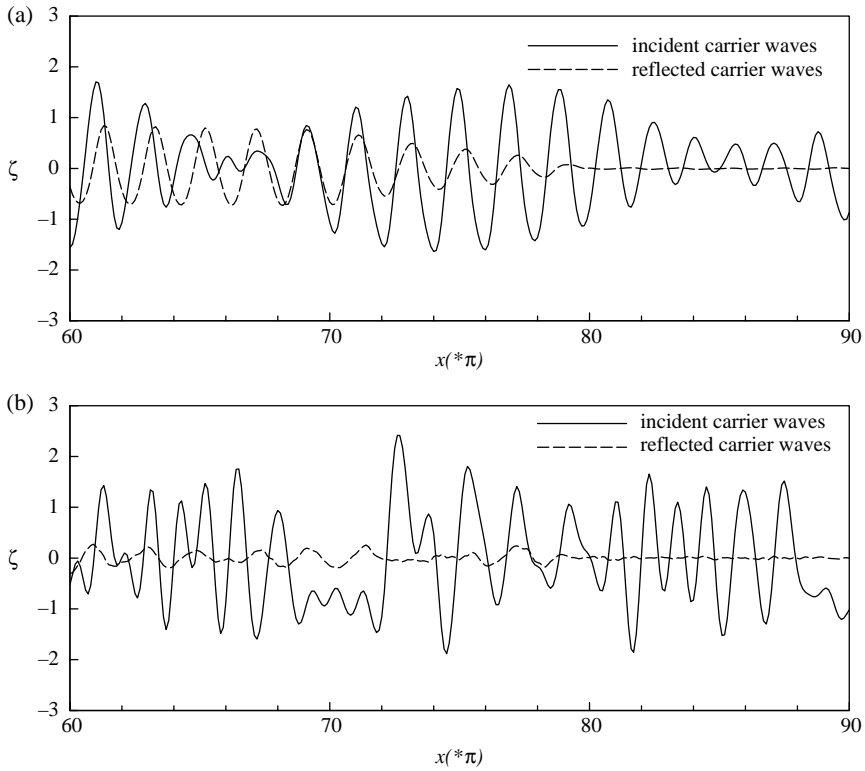


Fig. 4. Incident and reflected carrier waves composing wave groups over a rippled seabed: (a)  $\epsilon=0.02, \mu^2=0.1$ ; (b)  $\epsilon=0.08, \mu^2=0.1$ .

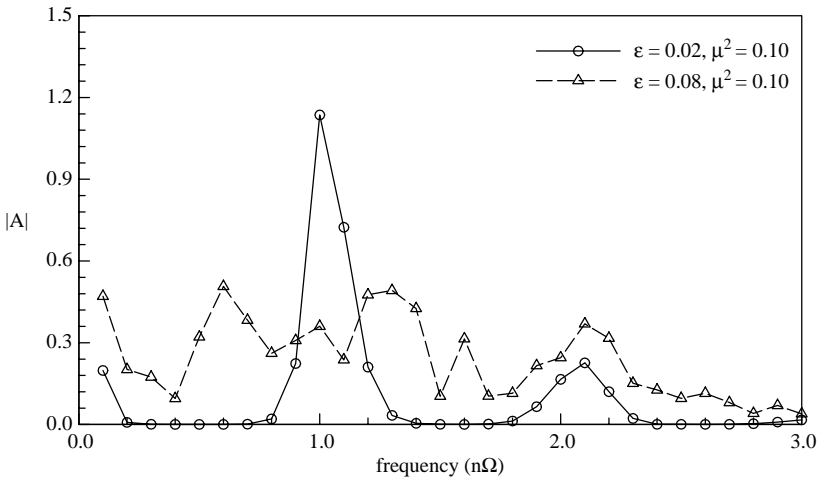


Fig. 5. The evolution of the amplitude spectrum of a wave group.

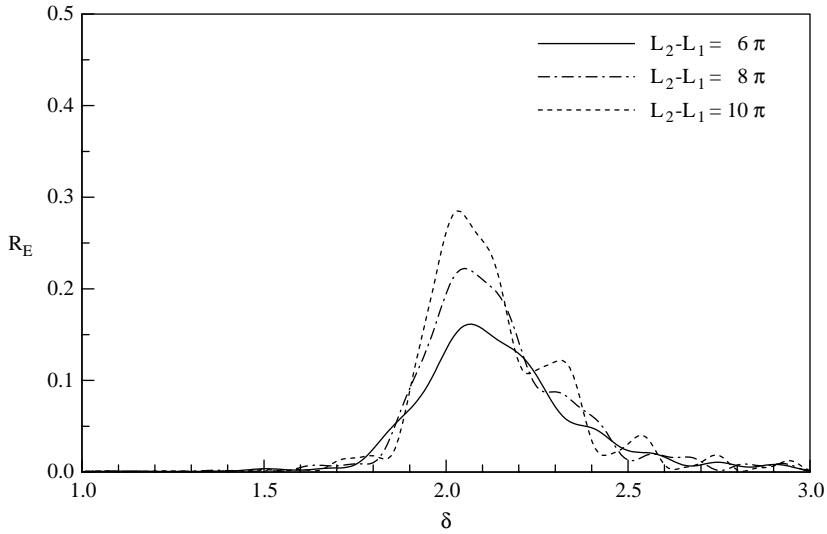


Fig. 6. Reflection coefficient of energy of carrier waves over a rippled bed ( $p=0.12$ ,  $\varepsilon=0.02$ ,  $\mu^2=0.1$ ).

the square of its amplitude. Thus, the reflection coefficient of wave energy could be expressed by

$$R_E = \frac{\sum_n |B_n|^2}{\sum_n |A_n|^2} \tag{26}$$

in which  $A_n$  and  $B_n$  represent incident and reflected wave components, respectively. In Fig. 6, the wave component with the angular frequency of  $n\Omega = 1.0$  is the largest. Thus,

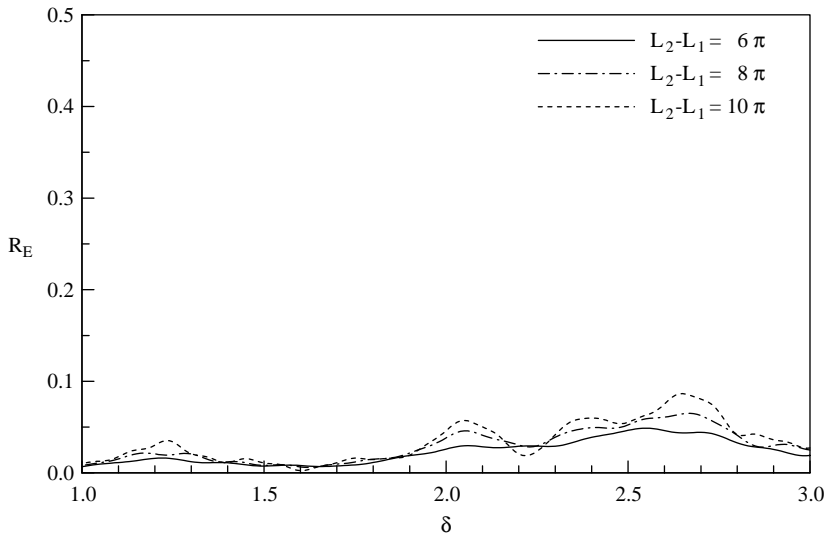


Fig. 7. Reflection coefficient of energy of carrier waves over a rippled bed ( $p=0.12$ ,  $\varepsilon=0.08$ ,  $\mu^2=0.1$ ).

a Bragg reflection occurs at  $\delta=2.6$ . In Fig. 7, wave components which have angular frequency of  $n\Omega = 1.2 \sim 1.4$  are large. The Bragg reflection occurs about at  $\delta=2$ . When the nonlinearity is relatively small, reflection coefficients increase largely at the Bragg reflection condition. However, the reflection coefficient of strong nonlinear waves change slightly as the wavenumber of a seabed varies. For conditions of  $\varepsilon=0.02$ ,  $\mu=0.1$ ,  $L_2-L_1=10\pi$  the reflected wave energy is about 30% of the incident wave energy at the Bragg reflection condition.

#### 4. Concluding remarks

In this paper, a set of governing equations is newly derived from the Boussinesq equations to investigate the evolution of wave groups and carrier waves composing wave groups over a sinusoidally varying topography. A splitting technique is used to derive the coupled nonlinear first-order ordinary differential equations describing transmitted and reflected wave fields.

The newly derived governing equations are then used to study the evolution of wave groups and Bragg resonant reflection of carrier waves. Incident waves are wave groups generated by two short waves with slightly different frequencies. The energy of the initial wave components is transferred to other harmonic components during propagation over a long distance. Evolution and reflection of short and long waves are influenced largely by nonlinearity. The reflection coefficient of carrier waves can be enhanced by decrease of nonlinearity.

#### References

- Arduin, F., Herbers, T.H.C., 2002. Bragg scattering of random surface gravity waves by irregular seabed topography. *J. Fluid Mech.* 451, 1–33.
- Bowers, E.C., 1977. Harbour resonance due to set-down beneath wave groups. *J. Fluid Mech.* 79, 71–92.
- Cho, Y.S., Lee, C.H., 2000. Resonant reflection of waves over sinusoidally varying topographies. *J. Coastal Res.* 16 (3), 870–876.
- Cho, Y.S., Lee, J.I., 2003. Resonant reflection of cnoidal waves on a sloping beach. *J. Coastal Res.* 19 (4), 1011–1017.
- Guazzelli, E., Rey, V., Belzons, M., 1992. Higher-order Bragg reflection of gravity surface waves by periodic beds. *J. Fluid Mech.* 245, 301–317.
- Heathershaw, A.D., 1982. Seabed-wave resonance and sand bar growth. *Nature* 296, 343–345.
- Kirby, J.T., 1986. A general wave equation for waves over rippled bed. *J. Fluid Mech.* 162, 171–186.
- Liu, P.L.F., Cho, Y.S., 1993. Bragg reflection of infragravity waves by sandbars. *J. Geophys. Res.* 98, 22733–22741.
- Liu, P.L.F., Yoon, S.B., Cho, Y.S., 1992. Shoaling of wave groups in shallow water. In: Debnath, L. (Ed.), *Nonlinear Dispersive Wave Systems*. World Scientific Publishing Co., pp. 41–56.
- Mei, C.C., Agnon, Y., 1989. Long-period oscillations in a harbour induced by incident short waves. *J. Fluid Mech.* 208, 595–608.
- Mei, C.C., Liu, P.L.F., 1993. Surface waves and coastal dynamics. *Ann. Rev. Fluid Mech.* 25, 215–240.
- Peregrine, D.H., 1967. Long waves on a beach. *J. Fluid Mech.* 25, 321–330.
- Yoon, S.B., Liu, P.L.F., 1987. Resonant reflection of shallow-water waves due to corrugated boundaries. *J. Fluid Mech.* 180, 451–469.